Modelling solar disability glare reflected off modern building facades

Matthew J. Glanville – CPP Pty Ltd, Sydney, Australia – mglanville@cppwind.com
Pallava R. Kodali – CPP Pty Ltd, Sydney, Australia – pkodali@cppwind.com
Mohammed Alsailani – CPP Inc, Windsor, USA – m.alsailani@gmail.com
Roberto P.M. Neto – CPP Pty Ltd, Sydney, Australia – rneto@cppwind.com

Abstract

Buildings can be examined during concept design to identify potential for sunlight to reflect off exterior cladding surfaces and create traffic disability glare onto surrounding roadways. Historically most assessment methodologies calculate veiling luminance hazard at roadway receiver locations assuming specular type reflections off glazing. A population dosage of veiling luminance is proposed in this paper as a disability glare risk measure. Modern facades are increasingly adopting metal sheet cladding products displaying both specular and highly diffuse reflective properties. In-house software has been developed to perform solar reflection calculations off a range of specular and diffuse reflective surface finishes. The program generates view-based luminance renderings at traffic receiver locations. Subsequently, a custom script evaluates the renderings and determines annual disability glare metrics including retinal irradiance, glare source angle and background luminance for comparison with existing disability glare criteria. Threshold increment is calculated from modelled veiling and background luminance as a measure of reduction in contrast due to disability glare. Case studies are reviewed where façade solar reflections flagged during early design as a traffic disability glare population dosage risk were successfully mitigated with façade treatments. Implications of façade solar reflectivity mitigation for building energy consumption are discussed.

1. Introduction

Sun disability glare occurs when direct or reflected sunlight is projected onto the retina of the human eye causing poor visibility. When driving it interferes with contrast, sharpness perception and vision acuity. Most motorists have experienced disability glare associated with driving directly toward a sunrise or sunset and these occurrences have been directly linked to grim accident and fatality statistics, e.g., (Mitra, 2014), (Sun et al., 2017), (Redelmeier et al., 2017) and (The Sunday Times, 2014). In terms of driver liability however the "Act of God" sun glare defence has been overruled in several legal cases given there should be some driver expectation of low altitude sun glare hazard being a natural event, e.g., (Dubois Law Group, 2012). It has been argued the driver should anticipate the hazard and take precautions by reducing speed, lowering sun visor, wearing sunglasses etc. Solar reflections from building facades however can be unexpected and come from unnatural and unexpected directions. Emergency doctrine may be a defence for a driver impacted by these unnatural solar reflections resulting from an "Act of the Designer".

Increasing urbanization in many cities is leading to higher traffic volumes exposed to reflected solar disability glare hazard and therefore increased community risk. As buildings become taller, so too do the distances over which low altitude reflected sun can cast onto surrounding roadways thereby increasing population dosage of reflected solar disability glare events.

Buildings can be examined during concept design to identify and quantify disability glare hazard onto surrounding roadways. Unfortunately, there has been little in the way of solar disability glare criterion for city planning consent authorities to prescribe and a need to further develop criteria and tools is recognised, e.g., (Danks et al., 2016) and (Glanville et al., 2024). Some of the earliest traffic glare assessment methodologies developed calculate Holladay veiling luminance L_v at receiver locations assuming specular type façade reflections.

2. Specular solar reflections

Building glazing products typically have specular solar reflectivity properties whereby the angle of incident sun ray onto the glass is equal to reflected solar ray angle. A popular methodology to identify and quantify disability glare associated with specular solar reflections from glazed facades was developed by (Hassall, 1991). Hassall's methodology calculates the diurnal and seasonal solar path at any given location (longitude and latitude) and calculates specular reflections off the subject building façade orientation onto surrounding roadway receiver locations. Glazing reflectivity properties are incorporated into the analysis as obtained from available product data or photometric tests. Human eye sensitivity of the motorist is then quantified by the Holladay formula in Equation 1.

$$L_v = \frac{kE_G}{\theta^2} \quad (1)$$

Holladay calculates a veiling luminance hazard L_v experienced by a driver of sufficient intensity to scatter the retinal image; appearing like a 'veil' placed in front of the observer's line of sight. Hassall nominates 500 cd/m² as a reasonable magnitude of limiting veiling luminance.

E_G is the illumination of reflected glare onto the corneal plane and k (typically in the order 10) accounts for variables such as age and colour of the subject's eye, (Adrian, 1989), (CIE 140, 2019), (Jurado-Piña et al., 2009) and (Vos, 2003). Central to the calculation of veiling luminance is the angle between the glare source and the driver's line of sight θ. A narrow angle θ coinciding with a glare source closely aligned to the driver's *required* line of vision will result in a high veiling luminance value and is to be avoided or mitigated. Pedestrians are not usually restricted to the same line of sight requirement imposed on a high-speed moving vehicle and can normally divert their line of sight to increase the angle θ.

A Population Dosage (cd.s/m²) per solar reflection event per day is proposed, being the product of veiling luminance (cd/m²), exposed road length (m) divided by traffic average speed (m/s), all multiplied by the number of vehicles exposed to the glare event (number of moving vehicles passing per unit time multiplied by glare event duration) and fraction of time with clear skies; these shifting variables integrated over the duration of a reflection event. As a rule of thumb, a value of approximately $1x10^6$ cd.s/m² constant luminance or greater per day implies a high population dosage risk for a reflection event.

3. Diffuse solar reflections

Modern facades are increasingly adopting metal sheet cladding products displaying both specular and highly diffuse reflective properties, e.g. (BHP, 2022). Diffuse reflections occur when sun rays reflecting off a rough surface are scattered in many directions.

Disability glare impact of both specular and diffuse solar reflections can be quantified using potential ocular impacts and assessed against criteria developed by (Ho et al., 2011). The Ho criteria has been used to assess solar reflections from roof and ground mounted photovoltaic panels at airport locations cast onto landing aircraft and is adapted in this study to assess glare hazard onto roadways surrounding buildings with facade materials such as metal cladding.

The Ho methodology assesses the ocular hazard caused by glint or glare as a function of the intensity of the glare upon the eye (retinal irradiance) E_r in W/m² and the subtended glare source angle ω being the extent to which the glare occupies the receptor's field of vision, dependent on size and distance of the reflector glare source. The severity of the ocular hazard can be assessed against three criteria levels as will be discussed in Section 5.1.1.

In-house software has been developed by CPP based on an open-source ray tracing engine, RADIANCE, to perform solar reflection calculations off a range of user specified surface finishes with flat to complex curvatures. Commercially available ClimateStudio software uses the RADIANCE engine and generates view-based luminance High-Dynamic Range (HDR) renderings at specific locations which could impact road users. A Stereographic Fisheye setting is typically used to produce the views and render luminance during daytime at set time intervals (typically 1 minute) throughout the solar year (ClimateStudioDocs.com,

2024). These annual HDR images for user nominated high-risk driver locations/orientation are processed using RADIANCE's internal tool Evalglare (Radiance-Online.org, 2020). CPP's custom software parallelises and automates the Evalglare processing of thousands of high-quality luminance images to identify façade locations and times of the year causing maximum driver impact. CPP's software system is tuned to filter glare sources and approaching driver fields of view as discussed further in section 5.1.1.

Using the principle of 'Reverse' photometry (Nilsson, 2009) whereby viewing is the reverse of radiating, glare source luminance is taken as the glare source on the eye plane and multiplied by glare source size Ω in steradians (sr) which are also extracted from the HDR images of daylight simulations; a similar approach has also been adopted by (Jakubiec et al., 2014). The subtended angle of the glare source ω in rad is obtained from the relationship:

$$\omega = 2\cos^{-1}\left(1 - \frac{\Omega}{2\pi}\right) \quad (2)$$

Luminance efficacy K is used to convert light from photometric to radiometric values for irradiance analysis (e.g. 100 lm/W for a morning clear-sky scenario). Corneal irradiance E_c in W/m² is converted to retinal irradiance E_r through the following relationship with reference to Fig.1:

$$E_r = \tau E_c \left(\frac{d_p^2}{d_r^2}\right) \quad (3)$$

Where the eye focal length f=0.017 m, glare source size ω in rad, diameter of the image projected onto the retina d_r in m ($f\omega$), ocular transmission coefficient τ=0.5, and pupil diameter d_p=0.002 m.

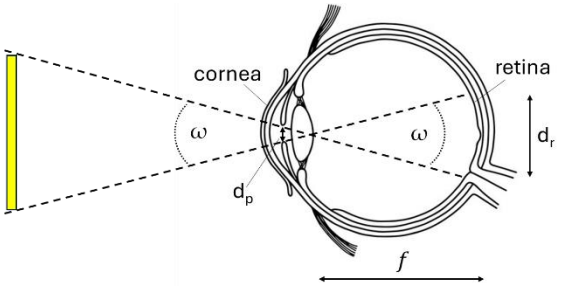

Fig. 1 – Section through the eye demonstrating a glare source projected onto the retina.

4. Contrast

Rod receptors on the retina of the eye at low light levels within the scotopic and into mesopic luminance range provide little colour response, provide low visual acuity but are highly sensitive to brightness and contrast (Armas et al., 2007). Hence contrast is an important measure of solar disability glare risk for a driver in mesopic dusk/dawn conditions and in some highly overcast or overshadowed daytime conditions. Threshold contrast for a target is given by:

$$C_b = \left(\frac{\Delta L}{L_b}\right) \quad (4)$$

Where:

$$\Delta L = L_t - L_b \quad (5)$$

L_t is the target luminance and L_b is the background luminance. Threshold contrast or Weber fraction (telescopeΘptics.net. 2023) varies with the type of physiological response. Extensive experiments were conducted by (Blackwell, 1946) to determine Contrast Threshold of the human eye under a variety of background luminance conditions. From this work a threshold contrast $C_b \approx 0.016$ would be suitable in the upper mesopic range up to background luminance with values of the order 10^2-10^3 cd/m².

Adding a veiling glare source L_v to both the target and background has the effect of reducing the effective contrast below threshold, Equation 6:

$$C_g = \frac{(L_t+L_v)-(L_b+L_v)}{L_b+L_v} = \frac{L_t-L_b}{L_b+L_v} \quad (6)$$

Scattering of light passing through atmospheric pollutants and windscreen media (dirt, water droplets, damage, and internal reflections) can be added to the veiling glare (Schreuder, 1991) and (Lundkvist et al., 1987).

Threshold Increment (TI) is defined as '*the measure of disability glare expressed as the percentage increase in contrast required between an object and its background for it to be seen equally well with the source of glare present*', (AS/NZS4282:2019). Within the scotopic to mesopic range limits of the code a '*higher value of TI corresponds to greater disability glare*.'

From the equations above it can be shown:

$$TI(\%) = \left(1 - \frac{C_g}{C_b}\right) \times 100 \quad (7)$$

Fechner (telescopeΘptics.net. 2023) noted departure from the Weber law at the extremes of perceived

brightness including retinal saturation at high luminance. In many instances the saturating background luminance associated with a low altitude solar disc will be in the same line of sight as a coinciding glancing façade reflection. In such conditions the low altitude sun can cast disability glare onto an approaching driver well exceeding a veiling luminance of 500 cd/m^2. With reference to the TI definition above however, the increase in contrast required between an object and the high background luminance due to the solar disc in the line of sight will not change significantly due to the veiling luminance of the façade reflection contribution. The façade contribution makes little difference to the driver disability glare event and hence a low TI value results. In this saturation luminance scenario the low TI value would be misleading in terms of a disability glare marker, however the low value demonstrates the negligible contribution from the building façade.

5. Case studies

5.1 Perpendicular reflections

Incident solar rays near perpendicular to a flat glazing plane with specular reflectivity properties will reflect solar rays with a veiling luminance of magnitude proportional to the visible light reflectivity coefficient of the glazing product.

5.1.1 Material selection for mitigation

CPP completed a solar disability glare study for the ICC Theatre in Sydney, Australia during the early planning stages. Mid-winter early morning rays were identified to strike the vertical east glazed façade with low altitude reflections back onto Pier Street westbound traffic travelling on an inclined roadway toward the site, Fig.2 (photo taken at nearby footpath location). Veiling luminance was predicted to be in the order 1100 cd/m^2 at approaching roadway locations using CPP in-house software following the Hassall methodology. The highest reflections were calculated off the southern end of the east façade initially modelled with a 10% visible light reflectivity coefficient glazing product.

Fig. 2 – Winter solstice morning solar reflection off Theatre east facade glazing - photograph courtesy Sydney Morning Herald.

A Population Dosage (cd.s/m^2) of approximately 1x10^6 cd.s/m^2 constant luminance per day was estimated for this reflection event and implies a population dosage risk.

View-based luminance renderings where prepared for further assessment of the 10% visible light reflectivity coefficient glazing product against the Ho criteria. Multiple potential reflective glare surfaces inside the driver's view field were assessed for both specular and diffuse reflections. Initial assessment of disability glare ignores the sky, direct sun, and the environment behind it to assess the net glare impact of the development. The software filters out these background contributions and calculates average luminance across an area exceeding a threshold luminance; the same area also defines subtended source angle. The initial result is plotted against the Ho criteria in Fig.3. The severity of the ocular hazard criteria is divided into three levels with the results in this example being marginally high at the low end of '*Potential for After-Images'*.

Glazing product selection with a low visible light reflectivity coefficient can be effective at mitigating these near perpendicular reflections. Reducing the visible light reflectivity coefficient of the glazing from 10% to just below 5% will reduce veiling luminance from 1100 cd/m^2 to the 500 cd/m^2 Hassall criteria and reduces reflections toward the Ho criteria for '*Low Potential for After Images*'

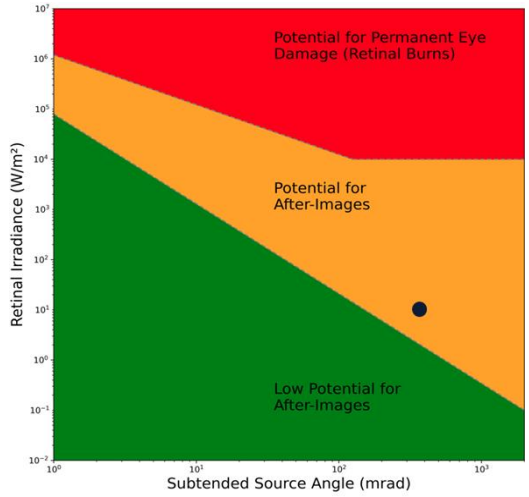

Fig. 3 – Potential impacts of retinal irradiance vs subtended source angle criteria by Ho et al. Result for winter solstice morning solar reflection off east facade glazing at roadway viewing position.

View-based luminance renderings are illustrated in Fig.4 with background contributions included. Concern remained in terms of contrast for an approaching driver during this mesopic dawn event, even with a <5% visible light reflectivity coefficient performance glazing product. In this example the software computes L_{20} = 1530 cd/m² background luminance as an area average in the 20° driver's field of view (white circle in Fig.4). Solving Equations 4 to 7 above for a veiling luminance meeting the Hassall limit L_v = 500 cd/m² gives a TI of 29% being marginally greater than suggested TI limits of 15-20%, e.g., (Armas et al., 2007), (AS/NZS1158.5:2014) and (AS/NZS 4282:2023).

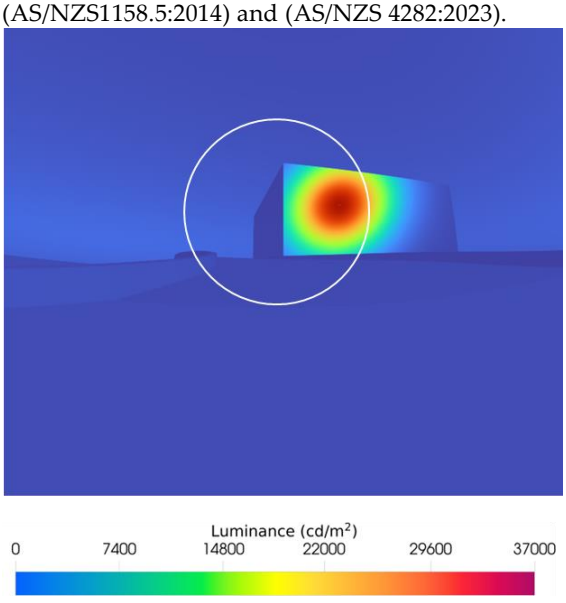

Fig. 4 – Winter solstice morning solar reflection off east facade glazing. View based luminance rendering at roadway viewing position.

Hence an alternative material was sought with a low reflectivity coefficient and diffuse reflective characteristics. A metal mesh product was selected for the southernmost 20 m of the east façade where there was greatest potential to reflect the morning sun toward the Pier Street roadway, Fig.5. The material has predominantly diffuse reflective properties producing reflections well below the codified TI limits.

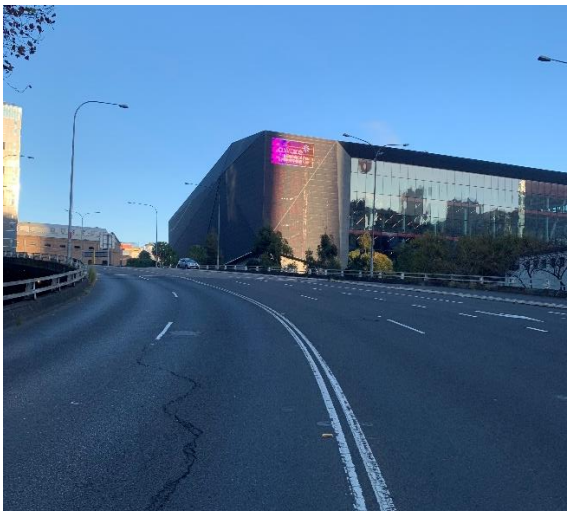

Fig. 5 – Winter solstice morning solar reflection off east facade metal cladding mesh. Photograph taken at the same simulated roadway viewing position.

Energy consumption for heating and cooling of a glazed façade building such as the ICC Theatre will be heavily dependent upon glass selection. The full spectrum of solar radiation reaching the facades will be either reflected by the glass (as measured by the solar energy reflectivity coefficient), transmitted directly into the building interior through the glass, or absorbed by the glass then re-released on the inner and outer glass surfaces. For most glazing products there is a close proportionality between the visible light reflectivity coefficient of the outer glass surface (important for glare studies) and the solar energy reflectivity coefficient. A low visible light reflectivity coefficient therefore generally means more solar radiation arriving at the glazing will penetrate the building and provide passive solar heating; being heavily dependent on the glass absorptance properties. Similarly, there will be some correlation between a higher visible light reflectivity coefficient glazing and lower cooling loads. Selection of specific glazing properties and products to reduce overall heating and cooling

loads is best made in conjunction with building energy simulation modelling.

5.1.2 Façade orientation for mitigation

Glazed balcony balustrades to a mid-rise Sydney apartment building were predicted to cast solar reflections toward oncoming traffic simultaneously over an extended stretch of highway in another example illustrated in Fig.6. At location 1 to the northeast of the balustrades, peak reflections with high veiling luminance were predicted during early morning traffic periods in early and late winter over a 100 m length of roadway representing a high population disability glare dosage. The straight length of roadway impacted was parallel to the reflected rays and inclined 1.6° toward the site resulting in very low θ values and hence high veiling luminance L_v over an extended receiver roadway length, limited almost only by building height.

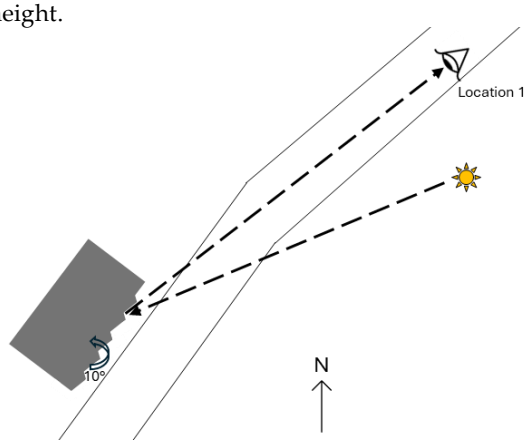

Fig. 6 – Perpendicular reflection example – mitigation by glazing reorientation.

In this example a simple reorientation of the northeast facing balustrade glazing by just 10° anticlockwise was sufficient to prevent the low altitude sun reflecting onto the this stretch of roadway.

5.2 Glancing reflections

Most glazing products will exhibit reflective properties of an ideal mirror when the incident and reflected solar rays are near parallel to the façade plane, i.e., a glancing reflection. Hence a glazed façade cannot be safeguarded just through low-reflectivity glass product selection and each building needs to be assessed considering façade orientation and alignment relative to oncoming traffic.

5.2.1 Opaque fins for mitigation

Glancing solar reflections are illustrated in Fig.7 for an early morning event at a Sydney location. The tall building façade is 25 m wide in plan and casts reflections towards drivers approaching the site from the west whereby the low altitude rising solar disc will approach the same line of sight as a coinciding glancing façade reflection. Planning authorities may require a low veiling luminance contribution from the facades of proposed buildings despite high pre-existing background luminance L_b as was discussed in Section 4.

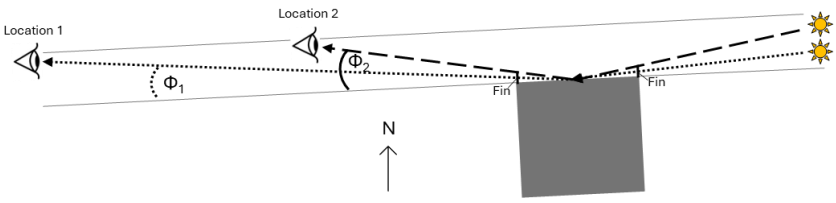

Fig. 7 – Glancing reflection example – mitigation by using vertical fins.

In Fig.7 it is the reflected rays closest to parallel to the façade that cast the highest veiling luminance onto eastbound drivers, and these can be readily blocked using opaque vertical fins placed perpendicular to the façade plane as illustrated in Fig.7. At location 1 to the west of the façade the peak veiling luminance reflection occurs just after sunrise in the mid-seasonal months at an angle Φ_1 reflected off a point on the façade 16m above ground level. The disability glare exceeds 500 cd/m² for 8 minutes over a 25 m length of flat roadway centred on location 1 and represents a population dosage risk during high volume traffic (similar but symmetrically reverse glancing solar reflections occur during afternoon traffic). Vertical fins placed with a fin depth to spacing ratio of 1:10 as illustrated in Fig.7 are sufficient to block incident and reflected rays of angle Φ_1 or shallower. At location 2 the same reflection event peaks half an hour later and here the fins are not deep enough to block a larger angle Φ_2. At this location the veiling luminance magnitude is significantly lower however due to a lager Φ_2 value contributing to the denominator of Equation 1. Furthermore, by blocking the earlier reflections the population dosage for the event is also significantly reduced.

In practice a series of much shallower fins having the same depth to spacing ratio can be implemented; the fins themselves should have a low-reflective finish. Alternatively, some forms of façade articulation can provide the same blockage effect, e.g. ratio of a punch window recess depth to window width. Solar shading associated with reflection mitigation can also be used to advantage in reducing building energy consumption particularly for cooling, e.g., angling vertical fins to shade low altitude summer sun.

6. Conclusions

This paper has reviewed an existing methodology to calculate traffic disability glare at roadway receiver locations resulting from specular type solar reflections off building glazing and proposes a population dosage of veiling luminance as a risk measure.

In-house software has been developed to perform solar reflection calculations off a range of specular and diffuse reflective surface finishes. The program generates view-based luminance renderings at traffic receiver locations. Subsequently, a custom script evaluates the renderings and determines annual disability glare metrics for comparison with existing disability glare criteria.

Threshold increment is calculated from the modelled veiling and background luminance as a measure of reduction in contrast due to disability glare.

Case studies are reviewed where façade solar reflections flagged during early design as a traffic disability glare population dosage risk were successfully mitigated with façade treatments. Implications of facade solar reflectivity mitigation for building energy consumption are discussed.

7. Acknowledgement

Solar disability glare consulting services at CPP Australia over almost two decades have also been supported by Kenneth Fung, Andrew Nguyen, Gemma Sibillin, Christopher Spencer and Joe Sun.

8. Nomenclature

Symbols

C_b	Threshold contrast
d_r	Diameter of an image projected onto the retina (m)
d_p	Daylight adjusted pupil diameter (m)
E_G	Corneal plane illuminance (lux or lm/m^2)
E_c	Corneal plane irradiance (W/m^2)
E_r	Retinal plane irradiance (W/m^2)
f	Eye focal length (~0.017 m)
k	10 by convention
K	Luminous efficacy (lm/W)
L_b	Background luminance (cd/m^2)
L_t	Target luminance (cd/m^2)
L_v	Veiling luminance (cd/m^2)
θ	Angle between the glare source and a receiver line of sight (°)
τ	Ocular transmission coefficient
Φ	Specular incident and reflected angle relative to façade in plan (°)
Ω	Subtended angle of glare source in steradians (sr)
ω	Subtended angle of glare source in radians (rad)

References

Adrian, I. W., 1989. "Visibility of targets: Model for calculation.", *Lighting Research and Technology*, Vol 21(4) 181-188. doi.org/10.1177/096032718902100404

Armas J., and J. Laugis. 2007. "Road Safety by Improved road lighting:road lighting measurements and analysis", *Topical problems of education in the field of electrical and power engineering*, 83-90.

Australian/New Zealand Standard, 2014. *Lighting for roads and public spaces Part 5: Tunnels and underpasses*, AS/NZS 1158.5:2014, Standards Australia.

Australian/New Zealand Standard, 2019. *Control of the obtrusive effects of outdoor lighting*, AS/NZS 4282:2019, Standards Australia.

Australian/New Zealand Standard, 2023. *Control of*

the obtrusive effects of outdoor lighting, AS/NZS 4282:2023, Standards Australia.

BHP, 2022. *Building Materials and Reflectivity*, Technical Bulletin TB-28 Rev 8. https://cdn.dcs.bluescope.com.au/download/tb-28

Blackwell, H. R., 1946. "Contrast Thresholds of the Human Eye.", *Journal of the Optical Society of America*, Vol 36 No. 11: 624-643. doi.org/10.1364/JOSA.36.000624

CIE 140, 2019. *Control of the obtrusive effects of outdoor lighting*, International Commission on Illumination, DOI: 10.25039/TR.140.2019

ClimateStudioDocs.com. 2024 "Radiance Render" ClimateStudio. Accessed 16 May 2024. https://climatestudiodocs.com/docs/radianceRender.html

Danks, R., J. Good, and R. Sinclair. 2016. "Assessing reflected sunlight from building facades: A literature review and proposed criteria.", *Journal of Building and Environment"*, Vol 103, 193-202. doi.org/10.1016/j.buildenv.2016.04.017

Dubois Law Group. 2012. "Drivers can still be held liable in sun glare car accidents." Accessed 17March2024. https://pdxinjurylaw.com/sun-glare/

Glanville, M.J., M. Alsailani, P.R. Kodali, and R.P.M. Neto. 2024. "Modelling Solar Reflections off Modern Building Facades", *CIE Australia Lighting Research Workshop 2024, Melbourne Eyecare Clinic*, The University of Melbourne, Abstract Booklet, p19.

Hassall, D. N. H., 1991. *Reflectivity: Dealing with Rogue Solar Reflections.* Faculty of Architecture, University of New South Wales.

Ho, C. K., C.M. Ghanbari and R.B. Diver. 2011. "Methodology to Assess Potential Glint and Glare Hazards from Concentrating Solar Power Plants: Analytical Models and Experimental Validation." *Journal of Solar Energy Engineering-Transactions of the ASME*, 133 (3). doi.org/10.1115/1.4004349

Jakubiec, J. A., and C. F. Reinhart. 2014. "Assessing Disability Glare Potential of Reflections from New Construction: Case Study Analysis and Recommendations for the Future." *Transportation Research Record: Journal of the Transportation Research Board*, Vol 2449, Issue 1. doi.org/10.3141/2449-13

Jurado-Piña, R., and J.M.P. Mayora. 2009. "Methodology to Predict Driver Vision Impairment Situations Caused by Sun Glare', *Transportation Research Record: Journal of the Transportation Research Board*, Vol. 2120, 12–17. doi.org/10.3141/2120-02

Lundkvist, S.O., G. Helmers, and S. Lofving. 1987. *Contrast Reductions in Windscreens*. Pilkington Sakerhetsgias AB, . Project no: 55316-4.

Mitra, S., 2014. "Sun glare and road safety: An empirical investigation of intersection crashes", *Safety Science*, Vol.70, 246–254 https://doi.org/10.1016/j.ssci.2014.06.005

Nilsson T.H., 2009. "Photometric specification of images", *Journal of Modern Optics,* Vol 56, 1523-1535. DOI: 10.1080/09500340902999263

Radiance-Online.org. 2020. "evalglare.pdf". Accessed 16 May 2024. https://www.radiance-online.org/learning/documentation/manual-pages/pdfs/evalglare.pdf/view

Redelmeier, D.A., and R. Sheharyar. 2017. "Life-threatening motor vehicle crashes in bright sunlight", *Medicine (Baltimore),* 96(1). doi: 10.1097/MD.0000000000005710.

Schreuder D.A., 1991. "Practical Determination of Tunnel Entrance Lighting Needs", *Transportation Research Record*. In TRB Annual Meeting, January.

Sun, D., K. El-Basyouny, and T.J. Kwon. 2017. "Sun Glare: Network Characterization and Safety Effects", *Transportation Research Record: Journal of the Transportation Research Board*, Vol. 2672 (16) 79–92. DOI:10.1177/0361198118784143

telescopeϴptics.net. 2023. "13.8. Eye Intensity Response, Contrast Sensitivity." Accessed 17March2024. https://www.telescope-optics.net/eye_intensity_response.htm

The Sunday Times. 2014. "News: Sun's Glare Causes 28 Road Deaths a Year" Accessed 17March2024. https://www.driving.co.uk/news/news-suns-glare-causes-28-road-deaths-a-year/

Vos, J.J., 2003. "On the cause of disability glare and its dependence on glare angle, age and ocular pigmentation", *Clinical and Experimental Optometry*, Vol86: Issue6: 363-370. doi.org/10.1111/j.1444-0938.2003.tb03080.x